Improved Parameter Estimation of Three-Phase Squirrel-Cage Induction Motors Using the Nelder-Mead Simplex Algorithm

Original Scientific Paper

Son T. Nguyen*
Hanoi University of Science and Technology,
School of Electrical and Electronic Engineering
Dai Co Viet Street, Hanoi, Vietnam
son.nguyenthanh@hust.edu.vn

Tu M. Pham
Hanoi University of Science and Technology,
School of Electrical and Electronic Engineering
Dai Co Viet Street, Hanoi, Vietnam
tu.phamminh@hust.edu.vn

Linh V. Trieu
Hanoi University of Science and Technology,
School of Electrical and Electronic Engineering
Dai Co Viet Street, Hanoi, Vietnam
linh.trieuviet@hust.edu.vn

Anh Hoang
Hanoi University of Science and Technology,
School of Electrical and Electronic Engineering
Dai Co Viet Street, Hanoi, Vietnam
anh.hoang@hust.edu.vn

*Corresponding author

Abstract *– This work presents a technique for precisely determining the characteristics of a squirrel-cage three-phase induction motor using the Nelder-Mead simplex algorithm. This approach is a frequently employed numerical optimization technique for determining the minimal value of a multi-dimensional objective function. An advantageous feature of the Nelder-Mead simplex algorithm is its independence from the need to calculate partial derivatives of the objective function. Nevertheless, similar to several optimization techniques, the Nelder-Mead simplex approach can also exhibit sensitivity to the initial conditions. Thus, the initial estimation of the parameters of the approximated equivalent circuit of the induction motor was used as the starting point for the Nelder-Mead optimization approach. The experiment's results are compared to those obtained using the polynomial regression approach to demonstrate the efficacy of the proposed method.*

Keywords: *three-phase induction motor, parameter estimation, the Nelder-Mead simplex algorithm*

Received: January 22, 2024; Received in revised form: June 14, 2024; Accepted: June 26, 2024

1. INTRODUCTION

Three-phase induction motors remain prevalent in many industrial applications due to their affordability, exceptional dependability, and uncomplicated design. The operating point of a three-phase induction motor can be determined by analyzing its equivalent circuit. Engineers can utilize the equivalent circuit to forecast the motor's behavior in different operating conditions, without taking into account the specific design characteristics of the motor. Nevertheless, manufacturers do not furnish the corresponding circuit parameters apart from the motor nameplate information, which encompasses the rated voltage, rated output power, efficiency, power factor, and rotor speed.

The three-phase induction motor's equivalent circuit has the following parameters: stator resistance, stator leakage inductance, core loss resistance, magnetizing inductance, rotor resistance with respect to the stator, and rotor leakage inductance with respect to the stator. The prevalent technique for determining the characteristics of a squirrel-cage induction motor relies on conducting no-load and locked rotor tests. Nevertheless, the locked rotor test poses certain difficulties due to the necessity of accurate voltage regulation and the use of appropriate equipment to securely immobilize the rotor in the locked position.

Manufacturers' nameplate data is valuable basic information for determining the equivalent circuit parameters of three-phase induction motors [1-3]. These efforts focused on developing non-iterative and iterative analytical approaches for solving simultaneous equations based on the motor parameters. Nevertheless, a significant limitation of these approaches is the absence of comprehensive nameplate data for all real three-phase induction motors. Furthermore, the motor characteristics can only be approximated in the absence of unpredictable variables, such as the alteration of stator and rotor winding resistances caused by an increase in temperature.

Typically, approaches for estimating the parameters of a three-phase induction motor can be categorized into two groups: offline estimation methods [4-9] and online estimation methods [10-12]. Typically, online estimations involve including power converters and additional controllers, followed by integrating the parameter estimation method into the control algorithm. Offline estimating methods necessitate fewer devices or operate without a controller, in contrast to online estimation methods.

The parameters of the three-phase motor can be calculated by utilizing data from various operational states of the motor. A phase-to-phase standstill variable frequency test was conducted in [4] to determine various operating modes of the motor. The test involved minimizing an error function by utilizing the measured resistance and reactance at different frequencies. Only the motors of the double-cage variant are appropriate for this technique. Different values of the load torque can be used to create various working conditions for a three-phase induction motor. A polynomial regression was then employed to solve the matrix equation formed by the partial derivatives of a cost function that is dependent on the input impedance of the motor's equivalent circuit [5, 6].

The motor parameters were computed using optimization algorithms such as the genetic algorithm (GA) [7, 8] and particle swarm optimization (PSO) [9]. The optimization approaches employed in the parameter estimation of three-phase induction motors are very responsive to initial circumstances. Without properly initialized parameters for the motor, the algorithm may produce undesirable outcomes. Currently, the field-oriented control (FOC) and direct-torque control (DTC) approaches are widely used for vector control of three-phase induction motors. If the parameters utilized for the motor do not align with the real motor specifications, the motor may not achieve the desired performance. The d-q model, which is commonly employed in vector induction motor control applications, is extensively utilized in the frequency domain [10]. A Luenberger observer [11] can be used to estimate the state variables and parameters of a three-phase induction motor concurrently. To achieve high-performance speed sensorless control of three-phase induction motors, it is necessary to make online estimations of the precise stator and rotor resistances. This is because these values can experience considerable increases because of the motor's temperature [12].

This paper introduces a comprehensive offline estimation procedure for determining the equivalent circuit parameters of a squirrel-cage three-phase induction motor in a laboratory setting. To determine the equivalent circuit parameters, it is necessary to measure the voltage, current, and active power of the motor input at various slip rates. The measurement system is straightforward, consisting solely of a single-phase electric meter and a digital rotational speed meter. The Nelder-Mead simplex algorithm [13, 14] is employed to minimize an objective function that is defined based on the discrepancy between the actual and estimated values of the input resistance and inductance of the precise equivalent circuit of the motor. To establish an appropriate beginning condition for the Nelder-Mead method, the initial motor parameters are derived by considering the approximate equivalent circuit of the motor. Subsequently, these characteristics are employed to determine the least value of the goal function associated with the precise equivalent circuit of the motor. This paper also includes a concise explanation of polynomial regression for motor parameter estimation, which serves to validate the efficacy of the proposed method.

The paper is structured in the following manner: Section 2 provides a concise overview of several equivalent circuits for three-phase induction motors and explains the process of determining the motor parameters using the estimated equivalent circuit. Section 3 provides a concise overview of how polynomial regression is employed to calculate the parameters of three-phase induction motors. Section 4 provides a thorough description of the Nelder-Mead simplex algorithm used for estimating the parameters of the three-phase induction motor. To verify the effectiveness of the proposed approach, an experimental setup is created and comprehensively explained in Section 5. The research findings are presented in Section 6.

2. EQUIVALENT CIRCUITS OF THREE-PHASE INDUCTION MOTORS

The equivalent circuit of a three-phase induction motor provides vital insights on the motor's performance. The comparable circuit of three-phase induction motors enables engineers to make critical decisions regarding design, operation, and efficiency enhancement. The equivalent circuit of an induction motor closely resembles that of a transformer since both devices facilitate the flow of energy from the primary to the secondary side. In the case of an induction motor, this energy transfer occurs from the stator side to the rotor side. Per-phase equivalent circuits of three-phase induction motors can be classified as follows:

- The exact per-phase equivalent circuit.
- The exact per-phase equivalent circuit without considering the magnetizing resistance.
- The approximate per-phase equivalent circuit.

2.1. THE EXACT PER-PHASE EQUIVALENT CIRCUIT

Fig. 1 shows the exact per-phase equivalent circuit of three-phase induction motors.

In which

- R_s : The stator winding resistance.
- X_s : The stator leakage reactance.
- R'_r : The rotor winding resistance referred to the stator side.
- X'_r : The rotor leakage reactance referred to the stator side.
- R_m : The magnetising resistance.
- X_m : The magnetising reactance.
- V_1 : The stator phase voltage.
- I_1 : The stator phase current.
- I_m : The magnetising current.
- I'_2 : The rotor current referred to the stator side.

To convert the rotor side parameters to the stator side, the rotor side parameters are divided by the square of a value K known as the effective rotor to stator turns per phase ratio.

$$R_r^{'} = \frac{R_r}{K^2} \quad (1)$$

$$X_r^{'} = \frac{X_r}{K^2} \quad (2)$$

The variables R_r and X_r represent the actual rotor resistance and the actual rotor leakage reactance, respectively. $R_r^{'}((1-s)/s)$ is a resistance that measures the amount of power transferred into mechanical power or the power that is useful.

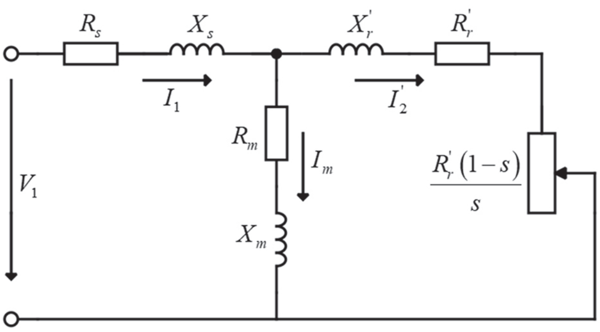

Fig. 1. The exact per-phase equivalent circuit of three-phase induction motors

2.2. THE EXACT PER-PHASE EQUIVALENT CIRCUIT IGNORING MAGNETISING RESISTANCE

Often, the magnetizing reactance is significantly more than the magnetizing resistance. The circuit depicted in Fig. 2 is obtained from the identical equivalent circuit shown in Fig. 1. The circuit depicted in Fig. 2 offers the benefit of facilitating the estimation of motor parameters through the utilization of the polynomial regression method, which will be discussed in Section 3.

2.3. THE APPROXIMATED PER-PHASE EQUIVALENT CIRCUIT

Fig. 3 depicts the estimated per-phase equivalent circuit, which is created by assuming a slight disparity between the supply voltage and the induced voltage. The approximate equivalent circuit is frequently employed to analyse the operational characteristics of three-phase induction motors in electric propulsion systems.

The parameters of the approximate equivalent circuit can be easily determined by conducting a direct current (DC) test, a no-load test, and a load test. The essential procedures for determining the values of the parameters in the approximate per-phase circuit are as follows:

- A DC test is conducted to directly quantify the resistance of the stator winding, denoted as R_s.
- A no-load test is conducted to calculate R_m and X_m.
- A load test is conducted using the data obtained from the no-load test in order to derive the values of R_r', X_s, and X_r'.

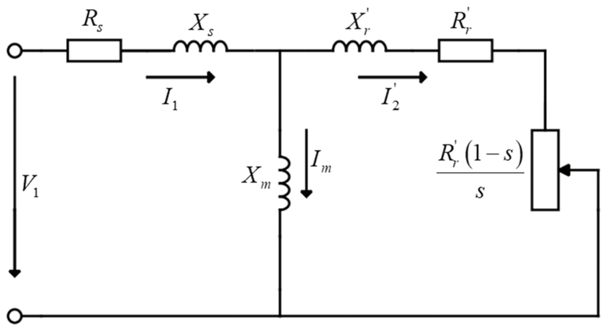

Fig. 2. The exact per-phase equivalent circuit of three-phase induction motors ignoring the magnetising resistance

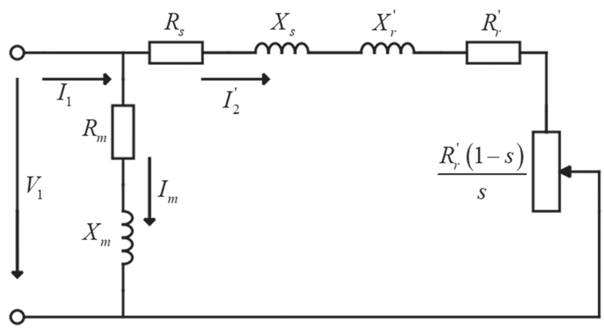

Fig. 3. The approximate per-phase equivalent circuit of three-phase induction motors

In the no-load test, the effects of the winding resistances and inductances are disregarded. Thus, just the component of the magnetizing resistance and inductance has persisted. The input impedance is expressed in the following manner:

$$Z_{in} = R_{in} + jX_{in} \tag{3}$$

$$R_m \approx R_{in} \tag{4}$$

$$X_m \approx X_{in} \tag{5}$$

The magnetising current is calculated as follows:

$$I_m = \frac{V_1}{R_m + jX_m} \tag{6}$$

The current in the winding branch is determined as follows:

$$I_2 = I_1 - I_m \tag{7}$$

The impedance of the winding branch is computed as follows:

$$Z_2 = \frac{V_1}{I_2} \tag{8}$$

The series connection of the resistors and inductors in the winding branch gives:

$$\mathrm{Re}(Z_2) = R_s + \frac{R_r^{'}}{s} \tag{9}$$

$$\mathrm{Im}(Z_2) = X_s + X_r^{'} \tag{10}$$

Using (9), R_r is determined as follows:

$$R_r = s\left(\mathrm{Re}(Z_2) - R_s\right) \tag{11}$$

Assuming $X_s \approx X_r'$ gives:

$$X_s = X_r^{'} = \frac{\mathrm{Im}(Z_2)}{2} \tag{12}$$

3. THREE-PHASE MOTOR PARAMETER ESTIMATION USING THE POLYNOMIAL REGRESSION

Polynomial regression can be employed to estimate the motor parameters by establishing the formula for the input impedance of the exact equivalent circuit, without considering the magnetizing resistance illustrated in Fig. 2.

$$Z = R_s + jX_s + \frac{jX_m\left(jX_r^{'} + \frac{R_r^{'}}{s}\right)}{jX_m + \left(jX_r^{'} + \frac{R_r^{'}}{s}\right)} \tag{13}$$

Equation (13) enables us to define an objective function by calculating the discrepancy between the n-th measured values and the n-th polynomial values in a straightforward manner.

$$E_n = R_n + jX_n - \frac{\left(a_0 + a_1 s_n + a_2 s_n^2\right) + j\left(a_3 + a_4 s_n^2\right)}{1 + b_2 s_n^2} \tag{14}$$

The n-th measured value of the slip rate is denoted by s_n. The coefficients a_0, a_1, a_3, a_4, and b_2 in equation (14) can be regarded as intermediate coefficients and are determined by:

$$a_0 = R_s;\ a_1 = \frac{X_m^2}{R_r^{'}};\ a_2 = R_s\frac{\left(X_m + X_r^{'}\right)^2}{R_r^{'2}};\ a_3 = X_s + X_m \tag{15}$$

$$a_4 = \frac{\left(X_s + X_m\right)\left(X_m + X_r^{'}\right)^2 - X_m^2\left(X_m + X_r^{'}\right)}{R_r^{'2}} \tag{16}$$

$$b_2 = \frac{\left(X_m + X_r^{'}\right)^2}{R_r^{'2}} \tag{17}$$

Re-arranging (14) gives:

$$E_n = \left[\frac{R_n\left(1 + b_2 s_n^2\right) - \left(a_0 + a_1 s_n + a_2 s_n^2\right)}{1 + b_2 s_n^2}\right] + j\left[\frac{X_n\left(1 + b_2 s_n^2\right) - \left(a_3 + a_4 s_n^2\right)}{1 + b_2 s_n^2}\right] \tag{18}$$

Equation (18) represents a combination of complex numbers. To minimize equation (18), it is necessary to establish an objective function with the following form:

$$S_E = \sum_{n=1}^{N}\left[R_n\left(1 + b_2 s_n^2\right) - \left(a_0 + a_1 s_n + a_2 s_n^2\right)\right]^2 + \left[X_n\left(1 + b_2 s_n^2\right) - \left(a_3 + a_4 s_n^2\right)\right]^2 \tag{19}$$

The concept of reactance distribution is presented by the utilization of the following ratio:

$$\eta = \frac{X_m + X_r^{'}}{X_m + X_s} \tag{20}$$

The range of values for η is between 0.95 and 1.05, and it may take multiple attempts to determine the appropriate ratio. By computing the partial derivatives of with S_E regard to b_2, a_0, a_1, a_2, a_3, and a_4, a matrix equation is derived, as depicted in equation (21). By solving this matrix equation, the values of b_2, a_0, a_1, a_2, a_3, and a_4, can be calculated. The motor parameters can then be found using equations (22) and (23).

4. THREE-PHASE MOTOR PARAMETER ESTIMATION USING THE NELDER-MEAD SIMPLEX ALGORITHM

4.1. OPTIMISATION PROBLEM FOR THREE-PHASE INDUCTION MOTOR PARAMETER ESTIMATION

The variables R_s, R_m, X_m, R_r, X_s, and $X_r^{'}$ can be determined by three measurement tests. These variables will then serve as the initial conditions for an optimization procedure aimed at enhancing the estimation of motor parameters. In the context of optimizing induction motor parameter estimates, it is necessary to create an objective function, as depicted in equation (24).

$$\begin{bmatrix} -\sum_{n=1}^{N}\left(R_n^2s_n^4+X_n^2s_n^4\right) & \sum_{n=1}^{N}\left(R_ns_n^2\right) & \sum_{n=1}^{N}\left(R_ns_n^3\right) & \sum_{n=1}^{N}\left(R_ns_n^4\right) & \sum_{n=1}^{N}\left(X_ns_n^2\right) & \sum_{n=1}^{N}\left(X_ns_n^4\right) \\ -\sum_{n=1}^{N}R_ns_n^2 & N & \sum_{n=1}^{N}s_n & \sum_{n=1}^{N}s_n^2 & 0 & 0 \\ -\sum_{n=1}^{N}R_ns_n^3 & \sum_{n=1}^{N}s_n & \sum_{n=1}^{N}s_n^2 & \sum_{n=1}^{N}s_n^3 & 0 & 0 \\ -\sum_{n=1}^{N}R_ns_n^4 & \sum_{n=1}^{N}s_n^2 & \sum_{n=1}^{N}s_n^3 & \sum_{n=1}^{N}s_n^4 & 0 & 0 \\ -\sum_{n=1}^{N}X_ns_n^2 & 0 & 0 & 0 & N & \sum_{n=1}^{N}s_n^2 \\ -\sum_{n=1}^{N}X_ns_n^4 & 0 & 0 & 0 & \sum_{n=1}^{N}s_n^2 & \sum_{n=1}^{N}s_n^4 \end{bmatrix} \begin{bmatrix} b_2 \\ a_0 \\ a_1 \\ a_2 \\ a_3 \\ a_4 \end{bmatrix} = \begin{bmatrix} \sum_{n=1}^{N}\left[R_n^2s_n^2+X_n^2s_n^2\right] \\ \sum_{i=1}^{N}R_n \\ \sum_{i=1}^{N}R_ns_n \\ \sum_{i=1}^{N}R_ns_n^2 \\ \sum_{i=1}^{N}X_n \\ \sum_{i=1}^{N}X_ns_n^2 \end{bmatrix} \quad (21)$$

$$X_m = \sqrt{\frac{\eta a_3\left(b_2a_3-a_4\right)}{b_2}};\ X_s = a_3 - X_m \quad (22)$$

$$X_r^{'} = \eta a_3 - X_m;\ R_r^{'} = \frac{X_m^2}{a_1} \quad (23)$$

$$S = \left|R_{in}-R\right|^2 + \left|X_{in}-X\right|^2 = f\left(R_s, R_m, X_m, X_s, X_r^{'}, R_r\right) \quad (24)$$

R_{in} and X_{in} represent the measured input resistance and inductance, respectively, of the exact equivalent circuit of the motor. The input resistance and inductance of the exact equivalent circuit of the motor determine its functionalities. These functions are contingent upon the variables of the motor parameters.

The input impedance of the exact per-phase equivalent circuit can be expressed as a function in the following manner:

$$Z = R_s + jX_s + \frac{\left(jX_m\right)\left(\frac{R_r^{'}}{s}+jX_r^{'}\right)}{\left(jX_m\right)+\left(\frac{R_r^{'}}{s}+jX_r^{'}\right)} \quad (25)$$

The input resistance and inductance are determined by the functions:

$$R = \mathrm{Re}\left(Z\right) \quad (26)$$

$$Z = \mathrm{Im}\left(Z\right) \quad (27)$$

4.2. THE NELDER-MEAD SIMPLEX ALGORITHM

The Nelder-Mead simplex algorithm can be elucidated by referencing Fig. 4 and performing the subsequent steps [13]:

1. A simplex has a set of points $x(i)$, $i=1,\ldots,n+1$.
2. The point in the simplex is ordered from the lowest function value $f(x(1))$ to the highest function value $f(x(n+1))$. In every step of the iteration, the current worst point $x(n+1)$ are discarded to accepts another point in the simplex.
3. Generate the reflect point:

$$r = 2m - x\left(n+1\right) \quad (28)$$

where $m = \sum_{i=1}^{n}\frac{x_i}{n}$ and calculate $f(r)$.

4. If $f(x(1)) \le f(r) < f(x(n))$, r is accepted and this iteration is stopped (**Reflect**).
5. If $f(r) < f(x(1))$, the expand point s is calculated as

$$s = m + 2\left(m - x\left(n+1\right)\right) \quad (29)$$

and f(s) is calculated.

   a. If $f(s) \le f(r)$, s is accepted and the iteration is stopped (**Expand**).

   b. Otherwise, r is accepted and the iteration is stopped (**Reflect**).

6. If $f(r) \ge f(x(n))$, a contraction is performed between m and the better of $x(n+1)$ and r.

   a. If $f(r) < f(x(n+1))$ (i.e., r is the better than $x(n+1)$, c is calculated as

$$c = m + \left(r - m\right)/2 \quad (30)$$

   and $f(c)$ is calculated.

   If $f(c) \le f(r)$, c is accepted and the iteration is stopped (**Contract outside**).

   Otherwise, Step 7 is continued (**Shrink**).

   b. If $f(r) \ge f(x(n+1))$, cc is calculate as

$$cc = m + \left(x\left(n+1\right) - m\right)/2 \quad (31)$$

   $f(cc)$ is calculated. If $f(cc) < f(x(n+1))$, cc is accepted and the iteration is stopped (**Contract inside**).

   Otherwise, Step 7 is continued (**Shrink**).

7. The n points are computed.

$$v\left(i\right) = x\left(1\right) + \left(x\left(i\right) - x\left(1\right)\right)/2 \quad (32)$$

   $f(v(i))$ is computed, $i=1,\ldots,n+1$. At the next iteration, the simplex consists of $x(1)$, $v(2),\ldots,v(n+1)$ (**Shrink**).

The figure below illustrates the points that are computed using the Nelder-Mead algorithm during the procedure.

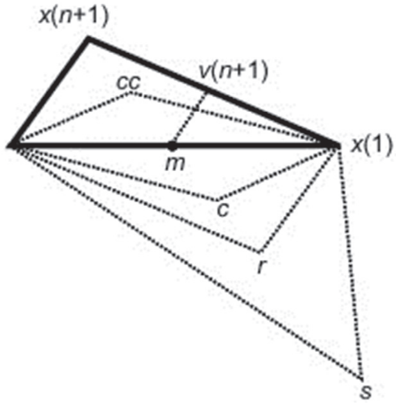

Fig. 4. The principle of generating points in a simplex

5. EXPERIMENTAL VALIDATION

Fig. 5 displays the experimental setup. The system comprises the following components:

- A 175W squirrel-cage three-phase induction motor manufactured by Lab-Volt company.
- A three-phase voltage source, 50Hz-220/380V, manufactured by Lab-Volt company.
- A dynamometer working as an adjustable load manufactured by Lab-Volt company.
- A single-phase electronic meter manufactured by LS company used to measure parameters of single-phase loads including the voltage, current and active power.

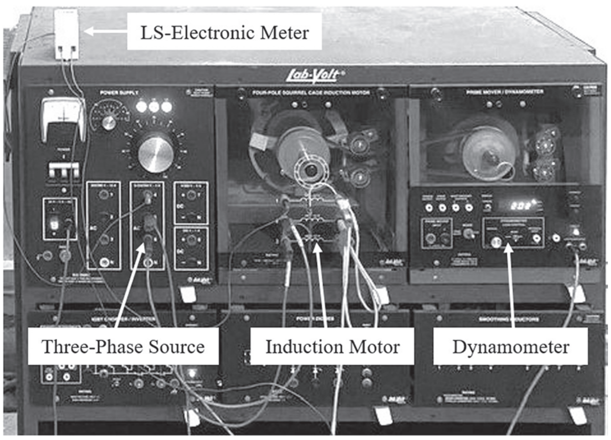

Fig. 5. The experimental setup.

5.1. THE POLYNOMIAL REGRESSION METHOD

Table 1 presents the recorded data for the speed, voltage, current, and active power of the motor at various load torque values. The dynamometer can be manually adjusted or modified by an external signal to achieve the appropriate load torque, which can vary between 0 and 1.5 (N.m). The per-phase voltage, current, and real power were recorded for a certain load torque value. Furthermore, the slip rate can also be determined by employing a digital speed meter.

Table 1. The collected data includes the rotor speed, per-phase voltage, current, and active power of the motor measured for various load torque values

TL (N.m)	Speed (rpm)	Voltage (Vrms)	Current (Arms)	Active Power (W)
0	1470	227.3	0.32	28
0.1	1457	227.3	0.34	31
0.2	1452	227.2	0.35	37
0.3	1445	226.9	0.37	43
0.4	1436	226.7	0.38	49
0.5	1427	226.6	0.4	55
0.6	1411	226.4	0.42	61
0.7	1404	226.5	0.44	68
0.8	1397	227.3	0.46	73
0.9	1385	227.4	0.49	79
1	1371	227.3	0.51	86
1.1	1360	227.1	0.54	92
1.2	1347	227.2	0.56	99
1.3	1338	227.2	0.59	106
1.4	1324	227.5	0.62	114
1.5	1311	227.5	0.66	125

The motor's speed, voltage, current, actual power, and slip rate were measured and utilized to estimate its electrical properties using the polynomial regression approach. Table 1 indicates that there are a total of 16 distinct instances of the operational states of the motor. The slip rate and input impedance of the motor are calculated using the following formulas:

$$s_n = \frac{n_1 - n_n}{n_1} \qquad n = 1,\ldots,16 \tag{33}$$

$$|Z_n| = \frac{V_n}{I_n} \qquad n = 1,\ldots,16 \tag{34}$$

$$R_n = \frac{P_n}{|I_n|^2} \qquad n = 1,\ldots,16 \tag{35}$$

$$X_n = \sqrt{|Z_n|^2 - R_n^2} \qquad n = 1,\ldots,16 \tag{36}$$

The slip rate, resistance, and reactance values of the motor, derived from equations (33), (35), and (36), are utilized in matrix equation (21) to obtain the motor parameters, as shown in Table 2. In this situation, the resistance caused by magnetization is ignored.

Table 2. Motor parameters estimated using the polynomial regression approach

R_s	X_s	X_m	R_r'	X_r'
47.8	57.5390	656.8813	52.9246	57.5390

5.2. THE NELDER-MEAD METHOD

To utilize the Nelder-Mead method for motor parameter estimation, it is necessary to possess an appropriate initial condition. To ensure ease, it is advisable to establish the beginning state by estimating the motor parameters from the approximate equivalent circuit. Under these conditions, it is necessary to do a DC test, a no-load test, and a load test.

A. DC Test

The DC test was conducted to measure the resistance of the stator winding. To conduct the test, a multi-meter can be used to measure the direct current (DC) resistance of the stator winding R_s=49(Ω).

B. No-Load Test

The no-load test was conducted to determine the values of the magnetizing resistance R_m and the magnetizing inductance X_m. Based on Table 1, the first case can be selected for the no-load test, using the following parameters:

- $V1$=227.3(V)
- $I1$=0.32(A)
- $P1$="28" (W)

The magnitude of the input impedance of the analogous circuit is determined by:

$$\left|Z_{in}\right| = \frac{V_1}{I_1} = \frac{227.3}{0.32} = 710.3125(\Omega) \tag{37}$$

The determination of the input resistance of the equivalent circuit is conducted in the following manner:

$$R_{in} = \frac{P_1}{I_1^2} = \frac{28}{0.32^2} = 273.4375(\Omega) \tag{38}$$

The input inductance of the equivalent circuit is determined by:

$$X_{in} = \sqrt{\left|Z_{in}\right|^2 - R_{in}^2} = \sqrt{710.3125^2 - 273.4375^2} = 655.5729(\Omega) \tag{39}$$

The magnetizing resistance and inductance can be determined in the following manner:

$$R_m = R_{in} = 273.4375(\Omega) \tag{40}$$

$$X_m = X_{in} = 655.5729(\Omega) \tag{41}$$

The calculation of the magnetizing current is as follows:

$$I_m = \frac{V_1}{R_m + jX_m} = \frac{227.3}{273.4375 + j655.5729} = 0.1232 - j0.2953(A) \tag{42}$$

C. Load Test

A load test was conducted to measure the rotor winding resistance referred to the stator side R_r', as well as the stator leakage inductance X_s and the rotor leakage inductance referred to the stator side X_r'. Table 1 indicates that the load test can be one of the scenarios where the load torque is not equal to zero. Under these conditions, the operational state of the motor was evaluated in relation to a load torque of 1.5 (N.m) using the following parameters:

- V_1=227.5(V)
- I_1=0.66(A)
- P_1="125" (W)
- n="1311" (rpm)

The magnitude of the input impedance of the equivalent circuit is calculated as follows:

$$\left|Z_{in}\right| = \frac{V_1}{I_1} = \frac{227.5}{0.66} = 344.6970(\Omega) \tag{43}$$

The circuit's input resistance is determined by:

$$R_{in} = \frac{P_1}{I_1^2} = \frac{125}{0.66^2} = 286.9605(\Omega) \tag{44}$$

The circuit's input inductance is determined by:

$$X_{in} = \sqrt{\left|Z_{in}\right|^2 - R_{in}^2} = \sqrt{344.6970^2 - 286.9605^2} = 190.9703(\Omega) \tag{45}$$

The input current of the equivalent circuit is calculated as follows:

$$I_1 = \frac{V_1}{Z_{in}} = \frac{227.5}{286.9605 + j190.9703} = 0.5495 - j0.3657(A) \tag{46}$$

The current flowing through the branch of the stator winding and rotor winding referred to the stator side is determined using the following calculation:

$$I_2 = I_1 - I_m = 0.4263 - j0.0703(A) \tag{47}$$

The impedance of the branch of the stator winding and rotor winding referred to the stator side is calculated in the following manner:

$$Z_2 = \frac{V_1}{I_2} = \frac{227.3}{0.4263 - j0.0703} = 519.57{+}j85.707(\Omega) \tag{48}$$

The slip rate is calculated as follows:

$$s = \frac{n_1 - n}{n_1} = \frac{1500 - 1311}{1500} = 0.126 \tag{49}$$

The calculation for the rotor winding resistance referred to the stator side is as follows:

$$R_r' = \left(\mathrm{Re}(Z_2) - R_s\right)s = (519.57 - 47.8) \times 0.126 = 59.4426(\Omega) \tag{50}$$

The stator leakage reactance and rotor leakage reactance referred to the stator side are calculated using the following formulas:

$$X_s = X_r' = \frac{\mathrm{Img}(Z_2)}{2} = \frac{85.707}{2} = 42.8536(\Omega) \tag{51}$$

The estimated values of R_s, R_m, X_m, X_s, X_r', *and* R_r' obtained from the approximate equivalent circuit were subsequently employed as the initial parameters for the optimization problem, aiming to directly determine the final values of the motor parameters using the exact equivalent circuit. Fig. 6 depicts the step-by-step process of the Nelder-Mead algorithm during the initial twenty rounds.

Table 3 displays the starting and end values of the motor parameters. Table 4 includes a statement of the comparison between the polynomial approach and the Nelder-Mead method. The Nelder-Mead approach offers the benefit of being able to determine all the parameters of the exact equivalent circuit.

5.3. MECHANICAL MOTOR PARAMETER ESTIMATION

The preceding sections provide a detailed explanation of the process for determining the electrical characteristics of an induction motor. The inertia moment *J* and the friction factor *F* of the motor can be estimated by a dynamic simulation, using pre-defined electrical parameters.

Fig. 7 depicts the simulation of the three-phase induction motor using Simulink. The moment of inertia *J* and the coefficient of friction of the motor *F* can be approximated by analysing the motor's start-up and the stable condition of the rotor's speed. The parameters of and can be iteratively adjusted multiple times until the simulated and actual motor speeds converge. The ultimate values of the mechanical parameters of the motor are *J*=0.001(kg.m^2) and *F*=0.0032(N.m.s).

Fig. 8 displays the rotor speed and electromagnetic torque during the motor's start-up. Table 5 presents a comparison of the simulated and measured values for the motor's voltage, current, and real power. The simulated values of the motor voltage, current, and real power closely match the measured values of the motor voltage, current, and real power. Table 6 displays the rated motor voltage, current, power factor, and efficiency for a motor with a mechanical power rating of 175 W.

```
Iteration   Func-count      min f(x)        Procedure
    0            1           9348.63
    1            6           9321.64        initial simplex
    2            8           4981.55        expand
    3            9           4981.55        reflect
    4           10           4981.55        reflect
    5           11           4981.55        reflect
    6           13            2477.1        expand
    7           15           393.079        expand
    8           16           393.079        reflect
    9           18           265.274        reflect
   10           20           8.69005        reflect
   11           21           8.69005        reflect
   12           23           8.69005        contract outside
   13           25           8.69005        contract inside
   14           27           8.69005        contract inside
   15           29           8.69005        contract outside
   16           31           8.69005        contract inside
   17           32           8.69005        reflect
   18           34           8.69005        contract inside
   19           36           8.69005        contract inside
   20           38           8.69005        contract inside
```

Fig. 6. The Nelder-Mead algorithm executed for the first twenty iterations

Table 3. Parameters of the exact equivalent circuit estimated using the Nelder-Mead method

Parameters	Initial Values	Final Values
R_s (Ω)	47.8	53.6589
X_m (Ω)	655.7729	685.8604
X_s (Ω)	42.8536	45.7919
X_r' (Ω)	42.8536	47.5990
R_r'(Ω)	59.4426	39.8770

Table 4. Parameters of the exact equivalent circuit estimated using the polynomial regression and the Nelder-Mead method

Parameters	Polynomial Regression Method	The Nelder-Mead Method
R_s (Ω)	47.8	53.6589
X_m (Ω)	656.8813	685.8604
X_s (Ω)	57.5390	45.7919
X_r' (Ω)	57.5390	47.5990
R_r'(Ω)	52.9246	39.8770

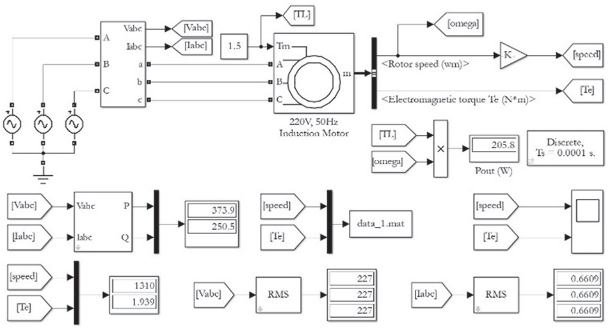

Fig. 7. Dynamic simulation of the three-phase induction in Simulink

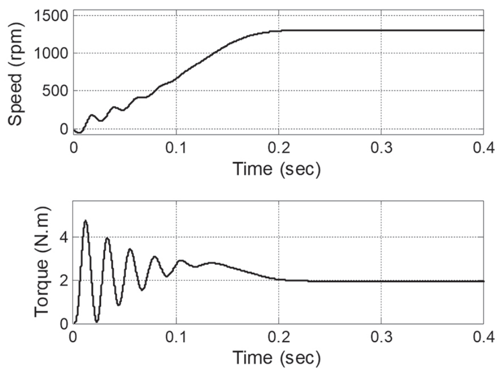

Fig. 8. Rotor speed and electromagnetic torque during the motor start-up

Table 5. Simulated and measured values of the motor voltage and current

TL (N.m)	Estimated Values		Measured Values	
	V (V)	I (A)	V (V)	I (A)
0	227	0.3287	227.3	0.32
0.1	227	0.339	227.3	0.34
0.2	227	0.3514	227.2	0.35
0.3	227	0.3657	226.9	0.37
0.4	227	0.3818	226.7	0.38
0.5	227	0.3996	226.6	0.40
0.6	227	0.4191	226.4	0.42
0.7	227	0.4401	226.5	0.44
0.8	227	0.4625	227.3	0.46
0.9	227	0.4865	227.4	0.49
1.0	227	0.5118	227.3	0.51
1.1	227	0.5386	227.1	0.54
1.2	227	0.5669	227.2	0.56
1.3	227	0.5966	227.2	0.59
1.4	227	0.6279	227.5	0.62
1.5	227	0.6609	227.5	0.66

Table 6. The rated motor voltage, current, real power, power factor, and efficiency

Phase Voltage (V)	220
Phase Current (A)	0.59
Output Power (W)	175
Power Factor	0.78
Efficiency (%)	56.69

6. CONCLUSIONS

The study outlines a comprehensive methodology for accurately determining the specifications of a three-phase induction motor that is not already in use. An efficient approach can be employed by utilizing a basic experimental setup and applying the Nelder-Mead simplex algorithm, a derivative-free optimization method. The Nelder-Mead method is initialized using the approximate equivalent circuit of the motor. Afterwards, the parameters of the exact equivalent circuit are estimated by minimizing a cost function that represents the discrepancy between the measured and estimated input impedance of the equivalent circuit. The Nelder-Mead simplex algorithm enables the calculation of all parameters of the exact equivalent circuit of the motor, without relying on assumptions like the reactance distribution ratio. This contrasts with the polynomial regression technique. The method suggested in this paper can also be applied to estimate parameters of single-phase induction motors. In terms of future research, the study intends to investigate the influence of temperature increase in the stator and rotor windings on the estimate of motor parameters required for the efficient control of three-phase induction motors using high-performance vector control.

7. ACKNOWLEDGEMENTS

This research is funded by Hanoi University of Science and Technology (HUST) under project number T2023-PC-041.

8. REFERENCES

[1] G. F. V. Amaral, J. M. R. Baccarini, F. C. R. Coelho, L. M. Rabelo, "A High Precision Method for Induction Machine Parameters Estimation From Manufacturer Data", IEEE Transactions on Energy Conversion, Vol. 36, No. 2, 2021, pp. 1226-1233.

[2] K. Lee, S. Frank, P. K. Sen, L. G. Polese, M. Alahmad, "Estimation of induction motor equivalent circuit parameters from nameplate data", Proceedings of the North American Power Symposium, Champaign, IL, USA, 9-11 September 2012.

[3] M. H. Haque, "Determination of NEMA Design Induction Motor Parameters From Manufacturer Data", IEEE Transactions on Energy Conversion, Vol. 23, No. 4, 2008, pp. 997-1004.

[4] L. Monjo, H. Kojooyan-Jafari, F. Córcoles, J. Pedra, "Squirrel-Cage Induction Motor Parameter Estimation Using a Variable Frequency Test", IEEE Transactions on Energy Conversion, Vol. 30, No. 2, 2015, pp. 550-557.

[5] R.-C. Wu, Y.-W. Tseng, C.-Y. Chen, "Estimating Parameters of the Induction Machine by the Polynomial Regression", Applied Sciences, Vol. 8, No. 7, 2018, p. 1073.

[6] S. T. Nguyen, S. Goetz, T. M. Pham, A. Hoang, T. V. Pham, "A Detailed Procedure of Squirrel-Cage Three-Phase Induction Motor Parameter Estimation Using Polynomial Regression", Proceedings of the 5th International Conference on Engineering Research and Applications, Thai Nguyen, Vietnam, 1-2 December 2022.

[7] K. S. Huang, Q. H. Wu, D. R. Turner, "Effective identification of induction motor parameters based on fewer measurements", IEEE Transactions on Energy Conversion, Vol. 7, No. 1, 2002, pp. 55-60.

[8] M. Z. Fortes, V. H. Ferreira, A. P. F. Coelho, "The Induction Motor Parameter Estimation Using Genetic Algorithm", IEEE Latin America Transactions, Vol. 11, No. 5, 2013, pp. 1273-1278.

[9] W.-M. Lin, T.-J. Su, R.-C. Wu, "Parameter Identification of Induction Machine With a Starting No-Load Low-Voltage Test", IEEE Transactions on Industrial Electronics, Vol. 59, No. 1, 2012, pp. 352-360.

[10] H. A. Toliyat, E. Levi, M. Raina, "A review of RFO induction motor parameter estimation techniques", IEEE Transactions on Energy Conversion, Vol. 18, No. 2, 2003, pp. 271-283.

[11] S. M. N. Hasan, I. Husain, "A Luenberger-Sliding Mode Observer for Online Parameter Estimation and Adaptation in High-Performance Induction Motor Drives", IEEE Transactions on Industry Applications, Vol. 45, No. 2, 2009, pp. 772-781.

[12] B. Karanayil, M. F. Rahman, C. Grantham, "Online Stator and Rotor Resistance Estimation Scheme Using Artificial Neural Networks for Vector Controlled Speed Sensorless Induction Motor Drive", IEEE Transactions on Industrial Electronics, Vol. 54, No. 1, 2007, pp. 167-176.

[13] J. C. Lagarias, J. A. Reeds, M. H. Wright, P. E. Wright, "Convergence Properties of the Nelder-Mead Simplex Method in Low Dimensions", SIAM Journal of Optimization, Vol. 9, No. 1, 1998, pp. 112-147.

[14] F. Gao, L. Han, "Implementing the Nelder-Mead simplex algorithm with adaptive parameters", Computational Optimization and Applications, Vol. 51, 2012, pp. 259-277.